*Supplement of*

# Extreme warming rates affecting alpine areas in SW Europe deduced from algal lipids

Antonio García-Alix, et al.

*Correspondence to:* Antonio García-Alix (agalix@ugr.es

**This Suplement includes the following data:**

Supplementary Figures S1-S3
Supplementary Tables S1-S7
Supplementary References

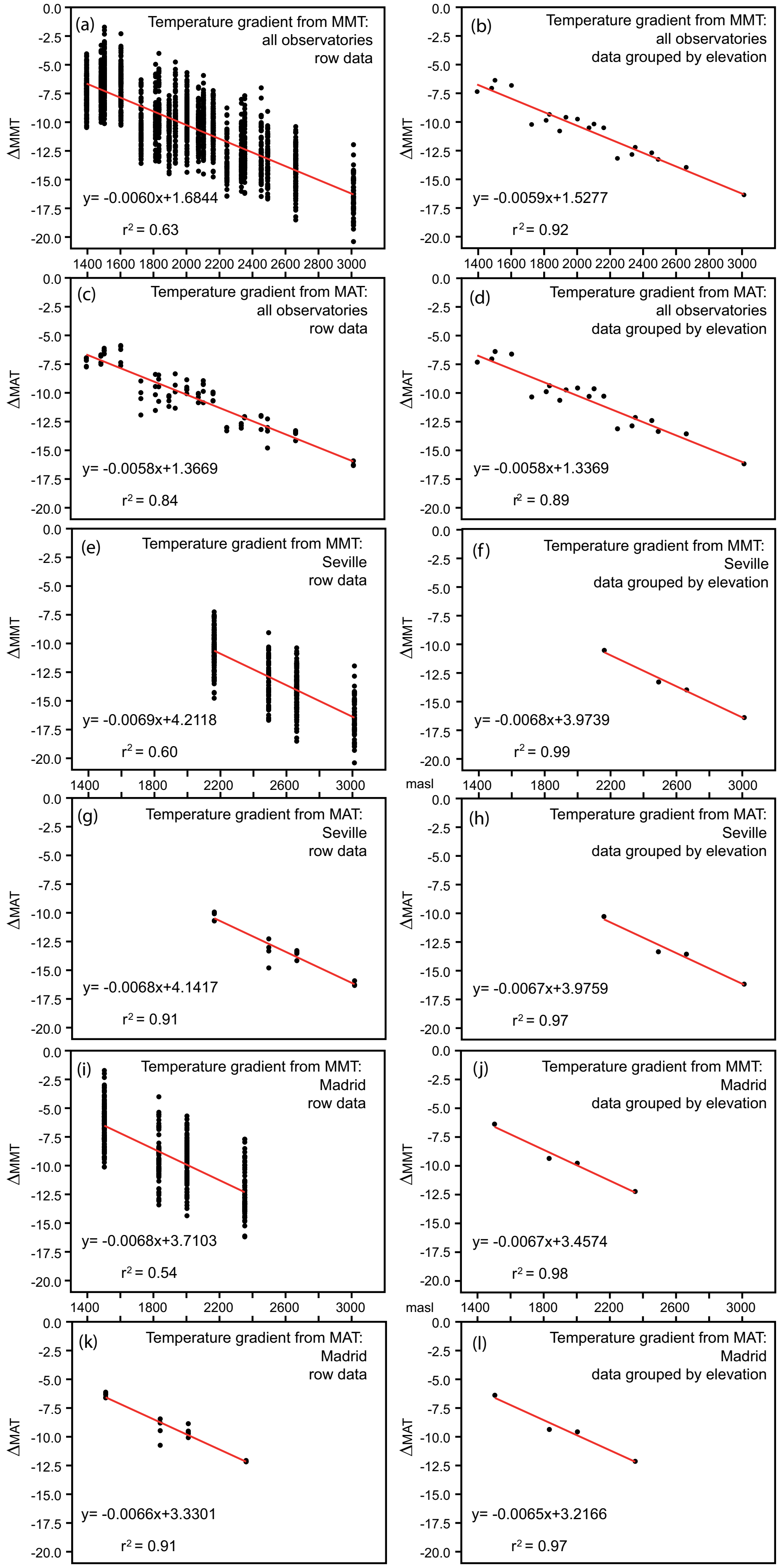

(a) Temperature gradient from MMT: all observatories row data
y= -0.0060x+1.6844
r² = 0.63
(b) Temperature gradient from MMT: all observatories data grouped by elevation
y= -0.0059x+1.5277
r² = 0.92
(c) Temperature gradient from MAT: all observatories row data
y= -0.0058x+1.3669
r² = 0.84
(d) Temperature gradient from MAT: all observatories data grouped by elevation
y= -0.0058x+1.3369
r² = 0.89
(e) Temperature gradient from MMT: Seville row data
y= -0.0069x+4.2118
r² = 0.60
(f) Temperature gradient from MMT: Seville data grouped by elevation
y= -0.0068x+3.9739
r² = 0.99
(g) Temperature gradient from MAT: Seville row data
y= -0.0068x+4.1417
r² = 0.91
(h) Temperature gradient from MAT: Seville data grouped by elevation
y= -0.0067x+3.9759
r² = 0.97
(i) Temperature gradient from MMT: Madrid row data
y= -0.0068x+3.7103
r² = 0.54
(j) Temperature gradient from MMT: Madrid data grouped by elevation
y= -0.0067x+3.4574
r² = 0.98
(k) Temperature gradient from MAT: Madrid row data
y= -0.0066x+3.3301
r² = 0.91
(l) Temperature gradient from MAT: Madrid data grouped by elevation
y= -0.0065x+3.2166
r² = 0.97
ΔMMT
ΔMAT
masl

**Supplementary Figure S1.** Calculation of the Environmental Lapse Rate (ELR, ºC/m) by means of Ordinary Least Square regressions from temperature and elevation variations ($\Delta_{elevation}$ and $\Delta_{MMT}$ or $\Delta_{MAT}$) between low and high elevation observatories listed in Table S1. Data from (Spanish National Weather Agency - AEMet Open Data, 2017;Gonzalez-Hidalgo et al., 2015;Observatorio del cambio global de Sierra Nevada, 2016). MMT (Monthly Mean Temperature) MAT (Mean Annual Temperature). (a) raw $\Delta_{MMT}$ vs $\Delta_{elevation}$ data (all observatories vs Sierra Nevada observatories); (b) mean $\Delta_{MMT}$ vs $\Delta_{elevation}$ data grouped by elevation (all observatories vs Sierra Nevada observatories); (c) raw $\Delta_{MAT}$ vs $\Delta_{elevation}$ data (all observatories vs Sierra Nevada observatories); (d) mean $\Delta_{MAT}$ vs $\Delta_{elevation}$ data grouped by elevation (all observatories vs Sierra Nevada observatories); (e) raw $\Delta_{MMT}$ vs $\Delta_{elevation}$ (Sevilla observatory vs. Sierra Nevada observatories); (f) mean $\Delta_{MMT}$ vs $\Delta_{elevation}$ (mean data grouped by elevation: Sevilla observatory vs. Sierra Nevada observatories); (g) raw $\Delta_{MAT}$ vs $\Delta_{elevation}$ (Sevilla observatory vs. Sierra Nevada observatories); (h) mean $\Delta_{MAT}$ vs $\Delta_{elevation}$ (mean data grouped by elevation: Sevilla observatory vs. Sierra Nevada observatories); (i) raw $\Delta_{MMT}$ vs $\Delta_{elevation}$ from (Madrid observatory vs. Sierra Nevada observatories); (j) mean $\Delta_{MMT}$ vs $\Delta_{elevation}$ (mean data grouped by elevation: Madrid observatory vs. Sierra Nevada observatories); (k) raw $\Delta_{MAT}$ vs $\Delta_{elevation}$ (Madrid observatory vs. Sierra Nevada observatories); (l) mean $\Delta_{MAT}$ vs $\Delta_{elevation}$ (mean data grouped by elevation: Madrid observatory vs. Sierra Nevada observatories). The obtained ERLs (ranging from 0.0058ºC/m to 0.0069ºC/m) are certainly close to the global mean ERL (~0.0065ºC/m) (Organization, 1993), showing that the different calculations are in agreement with the global temperature-elevation gradients.

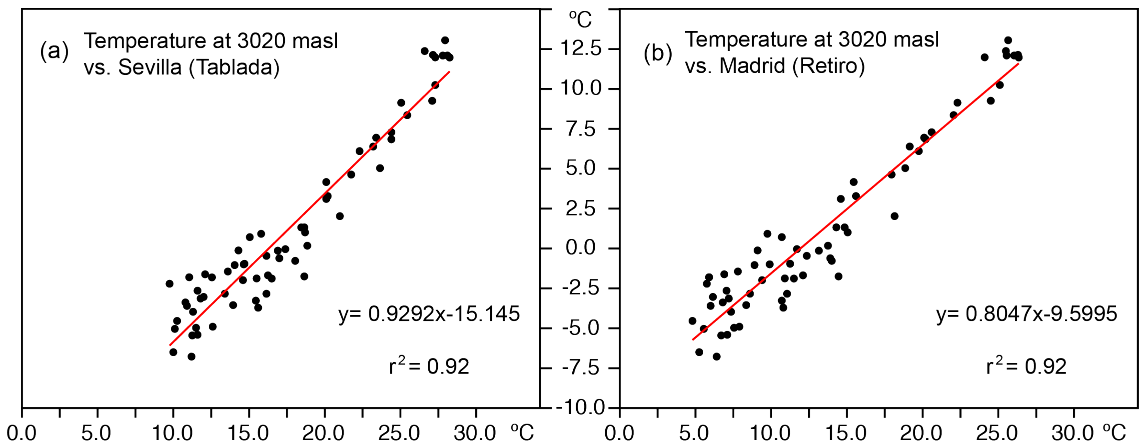


**Supplementary Figure S2.** (a) Correlation by means of Ordinary Least Square regression between Sevilla monthly temperatures and those from Cetursa 5 (3020 masl). (b) Correlations by means of Ordinary Least Square regression between Madrid monthly temperatures and those from Cetursa 5 (3020 masl). Data from (Spanish National Weather Agency - AEMet Open Data, 2017;Gonzalez-Hidalgo et al., 2015;Observatorio del cambio global de Sierra Nevada, 2016).

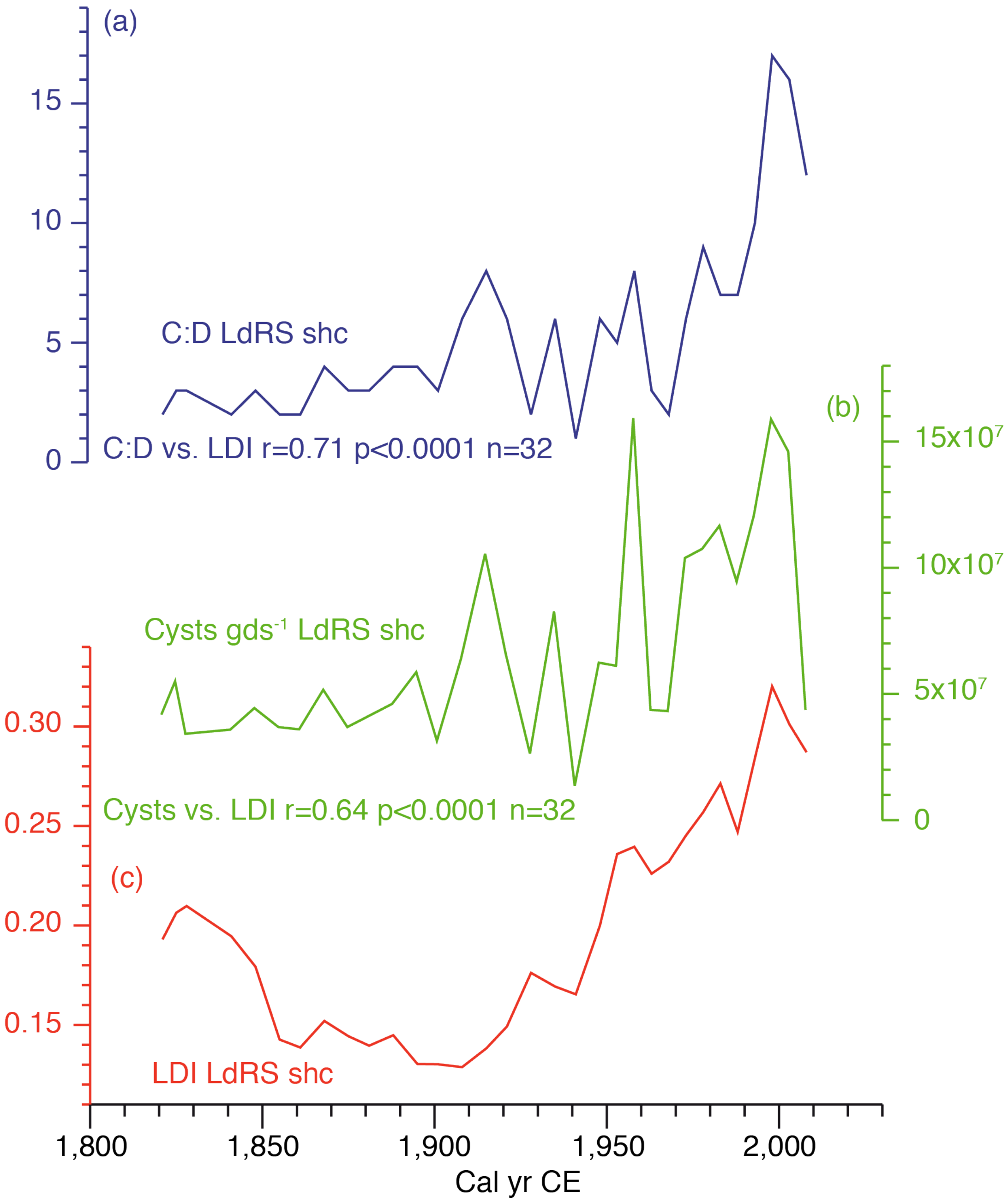


**Supplementary Figure S3.** Comparison between (a) the ratio of Chrysophyceae cysts (including *Chromulina* spp.) against the cysts + diatoms frustules (C:D), (b) the concentration of Chrysophyceae cysts per gram of dry sediment (cysts $gds^{-1}$), and (c) LDI in LdRS short core (LdRS shc), as well as their Pearson correlation (unpublished data from C. Pérez-Martínez). Interestingly, some Chrysophyceae algae produce resting siliceous cysts, more specifically *Chromulina nevadensis* and *Ochromonas* sp., two of the most abundant planktonic algae in Sierra Nevada lakes (Carrillo et al., 1991;Barea-Arco et al., 2001). There is a direct relationship between the amount of cysts produced and the number of live chrysophyte cells (Sandgren, 1988). The ratio between the cysts and the sum of cysts + diatoms frustules, as well as the number of cysts per gram of dry sediment (cysts $gds^{-1}$) in LdRS show a significant long-term Pearson correlation with the LDI ($r=0.71$-$0.72$ $p<0.0001$) and ($r=0.64$ $p<0.0001$) respectively. Since a statistically significant increasing trend has been observed in all the variables ($p<0.05$ in Mann-Kendall test), variables were transformed to the squares of the z-scores ($p<0.05$ in Mann-Kendall test for the LDI) and detrended, showing a significant Pearson correlation ($r=0.76$ $p<0.0001$) and ($r=0.45$ $p<0.01$) for the ratio between the cysts and the sum of cysts + diatoms frustules vs LDI and the number of cysts per gram of dry sediment (cysts $gds^{-1}$) vs LDI, respectively.

| Observatory | Observatory elevation (masl) | Sierra Nevada (SN) observatory | SN Observatory elevation (masl) | $\Delta_{elevation}$ (masl) |
|---|---|---|---|---|
| Sevilla (Tablada) | 8 | Albergue | 2500 | 2492 |
| Sevilla (Tablada) | 8 | Cetursa 1 | 2170 | 2162 |
| Sevilla (Tablada) | 8 | Cetursa 3 | 2670 | 2662 |
| Sevilla (Tablada) | 8 | Cetursa 5 | 3020 | 3012 |
| Granada Airport | 567 | Albergue | 2500 | 1933 |
| Granada Airport | 567 | Cetursa 1 | 2170 | 1603 |
| Granada Airport | 567 | Cetursa 3 | 2670 | 2103 |
| Granada Airport | 567 | Cetursa 5 | 3020 | 2453 |
| Madrid (Retiro) | 667 | Albergue | 2500 | 1733 |
| Madrid (Retiro) | 667 | Cetursa 1 | 2170 | 1503 |
| Madrid (Retiro) | 667 | Cetursa 3 | 2670 | 2003 |
| Madrid (Retiro) | 667 | Cetursa 5 | 3020 | 2353 |
| Granada Armilla | 687 | Albergue | 2500 | 1813 |
| Granada Armilla | 687 | Cetursa 1 | 2170 | 1483 |
| Granada Armilla | 687 | Cetursa 3 | 2670 | 1983 |
| Granada Armilla | 687 | Cetursa 5 | 3020 | 2333 |
| Granada Cartuja | 775 | Albergue | 2500 | 1725 |
| Granada Cartuja | 775 | Cetursa 1 | 2170 | 1395 |
| Granada Cartuja | 775 | Cetursa 3 | 2670 | 1895 |
| Granada Cartuja | 775 | Cetursa 5 | 3020 | 2245 |

**Supplementary Table S1**. Elevational difference between low and high elevation observatories used in this study

| Low vs high elevation observatories | Cetursa 5 3020 masl (n=67) | | Cetursa 3 2670 masl (n=113) | | Cetursa 1 2170 masl (n=121) | | Albergue 2500 masl (n=72) | |
|---|---|---|---|---|---|---|---|---|
| | *r* | *p* | *r* | *p* | *r* | *p* | *r* | *p* |
| **Madrid 667 masl** | 0.95920 | 7.99E-37 | 0.9671 | 8.28E-68 | 0.9641 | 2.44E-70 | 0.9598 | 2.40E-40 |
| **Sevilla 8 masl** | 0.95790 | 2.14E-36 | 0.9635 | 2.24E-65 | 0.9620 | 5.85E-69 | 0.9641 | 4.86E-42 |
| **Gr-Airport 567 masl** | 0.95430 | 2.80E-35 | 0.9655 | 4.18E-66 | 0.9626 | 8.66E-69 | 0.9591 | 4.37E-40 |
| **Gr-Cartuja 775 masl** | 0.96887 | 1.61E-40 | 0.9769 | 3.39E-76 | 0.9751 | 1.04E-79 | 0.9680 | 9.63E-44 |
| **Gr-Armilla 687 masl** | 0.96821 | 3.11E-40 | 0.9783 | 9.84E-78 | 0.9767 | 2.01E-81 | 0.9645 | 3.22E-42 |

**Supplementary Table S2.** Pearson correlations between MMT from low and high elevation (Sierra Nevada) observatories Data from (Spanish National Weather Agency - AEMet Open Data, 2017;Gonzalez-Hidalgo et al., 2015;Observatorio del cambio global de Sierra Nevada, 2016).The Mann-Kendall test performed using PAST software (Hammer et al., 2001) in the raw data of these variables showed a p>0.05 pointing towards no linear trends; so, no transformation has been applied.

| LDI vs Low elevation observatories | n | Normal correlation | | (z-score)$^2$ correlation | | Mann-Kendall | Detrended correlation | |
|---|---|---|---|---|---|---|---|---|
| | | ***r*** | ***p*** | ***r*** | ***p*** | ***no trend p>0.05*** | ***r*** | ***p*** |
| Sevilla MATA | 19 | 0.9092 | 7E-08 | 0.8926 | 2E-07 | 0.6746 | 0.9462 | 9E-10 |
| Sevilla MSTA | 19 | 0.7198 | 0.0005 | 0.2655 | 0.2719 | 0.0424 | 0.3957 | 0.0935 |
| Madrid MATA | 19 | 0.9074 | 8E-08 | 0.8383 | 7E-06 | 0.6746 | 0.9291 | 9E-09 |
| Madrid MSTA | 19 | 0.7662 | 0.0001 | 0.5071 | 0.0267 | 0.0863 | 0.6276 | 0.0040 |
| Gr-Airport MATA | 19 | 0.7056 | 0.0007 | 0.6338 | 0.0036 | 0.9998 | 0.7015 | 0.0008 |
| Gr-Airport MSTA | 19 | 0.5788 | 0.0094 | 0.3381 | 0.1568 | 0.1837 | 0.4247 | 0.0699 |
| Gr-Cartuja MATA | 19 | 0.7327 | 0.0004 | 0.6606 | 0.0021 | 0.5756 | 0.6927 | 0.0010 |
| Gr-Cartuja MSTA | 19 | 0.6477 | 0.0027 | 0.4080 | 0.0829 | 0.2939 | 0.4501 | 0.0532 |
| Gr-Armilla MATA | 19 | 0.6971 | 0.0009 | 0.6853 | 0.0012 | 0.8337 | 0.6934 | 0.0010 |
| Gr-Armilla MSTA | 19 | 0.6113 | 0.0054 | 0.3849 | 0.1037 | 0.3446 | 0.4067 | 0.0840 |

**Supplementary Table S3.** Pearson correlations (normal and detrended) for the last ~100 years among LdRS shc LDI and temperature time-series of different observatories. Normal correlations show the relationship between long-term trends. Data from (Spanish National Weather Agency - AEMet Open Data, 2017;Gonzalez-Hidalgo et al., 2015;Observatorio del cambio global de Sierra Nevada, 2016). Data were standardised (z-scores), normalised (squares) and a Mann-Kendall trend test was performed using PAST software (Hammer et al., 2001) in order to assess the existence of any trend over time in the data series. Afterwards, data were detrended by fitting a linear regression versus time, and a Pearson correlation was worked out with the residuals. Observatories: Granada city (~600-700 masl and 30km from LdRS), Madrid (Retiro: 667 masl and ~360km from LdRS) and Sevilla (Tablada: 8 masl and ~230km from LdRS but almost similar latitude as LdRS). Mean annual temperature anomaly (MATA) and mean warm season (May-September) temperature anomaly (MSTA) have been tested. MSTA have also been included in the comparison because warm season temperature (May-September) influences algae growth in the studied area (Sánchez-Castillo, 1988;Carrillo et al., 1991). The three time-series available from Granada city only have reliable data from the 1970s onwards (AEMet) (Spanish National Weather Agency - AEMet Open Data, 2017), what is too short for a proper proxy calibration. Longer temperature time-series have been obtained from these Granada series using different approaches to fill in gaps and correct outlying data; i.e. MOTEDAS approach (Gonzalez-Hidalgo et al., 2015). Even though these reconstructed temperatures from Granada for the last ~100 years show a good correlation with LDI (Gr-Airport $r>0.70$ Gr-Cartuja $r> 0.69$; Gr-Armilla $r>0.69$ $p<0.001$), they are likely biased by the quality of the reconstructed data. Besides, the quality of the records (presence of gaps), this discrepancy between LdRS LDI and Granada record series could be linked to the strong control of Granada basin geomorphology in local rain and temperature patterns at low elevations, with local clouds and frequent thermal inversion phenomena and specific microclimate. Madrid and Sevilla area are not influenced by this effect (Dogniaux, 1994).

| **$\Delta_{temperature}$ vs $\Delta_{elevation}$** | **$\Delta_{temp}$ from *eq b* (global $\Delta_{MMT}$)** | **$\Delta_{temp}$ from *eq d* (global $\Delta_{MAT}$)** | **$\Delta_{temp}$ from *eqs f and j* (MMT)** | **$\Delta_{temp}$ from *eqs h and l* (MAT)** | **Real $\Delta_{temp}$ from MMT** | **Real $\Delta_{temp}$ from MAT** |
|---|---|---|---|---|---|---|
| **Sevilla 8 masl** | 16.24 ºC | 16.13 ºC | 16.51 ºC | 16.20 ºC | 16.39 ºC | 16.17 ºC |
| **Madrid 667 masl** | 12.36 ºC | 12.31 ºC | 12.31 ºC | 12.08 ºC | 12.23 ºC | 12.14 ºC |

**Supplementary Table S4.** $\Delta_{temperature}$ between Madrid and Sevilla observatories and Cetursa5 (at the same elevation as LdRS, 3020 masl) worked out using different approaches: 1) using equation from Fig. S1b from the mean values between $\Delta_{MMT}$ and $\Delta_{elev}$ among all the studied low elevation observatories vs those from high elevation; 2) the same as the previous one but with the $\Delta_{MAT}$ (equation from Fig. S1d); 3) using equations from Fig. S1f and j (Sevilla-Madrid respectively) from the mean values between $\Delta_{MMT}$ and $\Delta_{elev}$ of Sevilla or Madrid observatories respectively vs those from high elevation; 4) the same as the previous one but with the $\Delta_{MAT}$ (equations from Fig. S1h and l); 5) real $\Delta_{MMT}$ between Sevilla or Madrid observatories and Cetursa 5 observatory (3020 masl); 6) the same as the previous one but with the $\Delta_{MAT}$.

| LdRS shc LDI vs | | n | Normal correlation | | $(z\text{-score})^2$ correaltion | | Mann-Kendall | Detrended correlation | |
|---|---|---|---|---|---|---|---|---|---|
| | | | *r* | *p* | *r* | *p* | *no trend $p>0.05$* | *r* | *p* |
| **Solar** | **ΔTSI** | 32 | 0.5850 | 0.0004 | -0.0992 | 0.5891 | 0.9611 | -0.0256 | 0.8893 |
| | **TSI** | 32 | 0.5570 | 0.0009 | 0.1050 | 0.5675 | 0.8711 | 0.0204 | 0.9120 |
| **Volcanic** | **NH volcanic aerosol** | 27 | -0.0200 | 0.9181 | -0.0561 | 0.7724 | 0.7196 | 0.0892 | 0.7724 |
| | **Global volcanic aerosol** | 27 | 0.0247 | 0.8987 | 0.1156 | 0.5505 | 0.9085 | 0.2062 | 0.5505 |
| | ***Global volcanic forcing** | 27 | 0.0843 | 0.7165 | 0.2099 | 0.2745 | 0.4365 | 0.3001 | 0.2745 |
| **Atmospheric** | **NAO** | 30 | -0.0281 | 0.8830 | 0.3276 | 0.0772 | 3E-05 | 0.0542 | 0.7760 |
| | **AMO** | 32 | 0.6097 | 0.0002 | 0.4063 | 0.0210 | 0.3724 | 0.3233 | 0.0711 |
| **Green house gases** | **$CO_2$ (ppm)** | 31 | 0.8328 | 6E-09 | 0.7655 | 5E-07 | 0.3587 | 0.7039 | 0.0000 |
| | **$NO_2$ (ppm)** | 31 | 0.8533 | 1E-09 | 0.7776 | 2E-07 | 0.4646 | 0.7134 | 0.0000 |
| | **$CH_4$ (ppm)** | 31 | 0.8610 | 5E-10 | 0.7346 | 2E-06 | 0.5633 | 0.6493 | 0.0001 |
| **Temperatures** | **CPS Summer temperatures** | 32 | 0.5775 | 0.0007 | 0.4406 | 0.0131 | 0.2998 | 0.3991 | 0.0261 |
| | **SST uk37 Gol-Ho1B** | 32 | 0.7601 | 4E-07 | 0.2386 | 0.1884 | 0.8330 | 0.1626 | 0.3739 |
| | **Global Temperatures (GLSS)** | 19 | 0.8898 | 3E-07 | 0.6920 | 0.0010 | 0.6243 | 0.7435 | 0.0003 |

**Supplementary Table S5.** Pearson correlations (normal and detrended) between LdRS short core LDI record and different proxies for solar and volcanic forcing, North Atlantic modes, greenhouse gases, and temperatures. Normal correlations show long-term trends. Data were standardised (z-scores), normalised (squares) and a Mann-Kendall trend test was performed using PAST software (Hammer et al., 2001) in order to assess the existence of any trend over time in the data series. Afterwards, data were detrended by fitting a linear regression versus time, and a Pearson correlation was worked out with the residuals. *: Note that inverse global volcanic forcing values have been used in order to show the same trends as in Fig. 5.

**Solar Proxies:** ΔTSI, reconstruction of the difference of the total solar irradiance from the value of the PMOD composite series during the solar cycle minimum of the year 1986 CE (1365.57 W $m^{-2}$) (Steinhilber et al., 2009); TSI, total solar Irradiance (Coddington et al., 2016).

**Volcanic proxies:** Annual stratospheric volcanic sulfate aerosol injection for the past 1500 years in the North Hemisphere and worldwide (Gao et al., 2008); global volcanic aerosol forcing (W $m^{-2}$) (Sigl et al., 2015).

**North Atlantic modes:** NAO, North Atlantic Oscillation reconstruction (Trouet et al., 2009); AMO, Atlantic Multidecadal Oscillation reconstruction (Mann et al., 2009).

**Greenhouse gases**: reconstructed concentrations of atmospheric $CO_2$, $NO_2$, and $CH_4$ (ppm) (Schmidt et al., 2011).

**Temperatures:** Composite-plus-scaling (CPS) mean summer temperature anomaly reconstruction from tree rings records in Europe with respect to 1974-2003 CE (MSTA ºC) (Luterbacher et al., 2016); Alkenone-Sea Surface Temperatures (SST ºC) of the core Gol-Ho1B_KSGC-31 (Gulf of Lion: NW Mediterranean Sea) (Sicre et al., 2016), and global land and sea surface (GLSS) mean annual temperature anomalies with respect to 1979-2008 CE (Hansen et al., 2010).

| LdRS lgc LDI vs | | n | Normal correlation | | $(\text{z-score})^2$ correaltion | | Mann-Kendall | Detrended correlation | |
|---|---|---|---|---|---|---|---|---|---|
| | | | *r* | *p* | *r* | *p* | *no trend* *$p>0.05$* | *r* | *p* |
| Solar | **$*\Delta^{14}C$** | 16 | -0.7260 | 0.0015 | 0.3949 | 0.1301 | 0.1917 | 0.3810 | 0.1454 |
| | **ΔTSI** | 20 | 0.6916 | 0.0007 | 0.3759 | 0.1024 | 0.0231 | 0.3668 | 0.1117 |
| | **TSI** | 13 | 0.8779 | 0.0001 | 0.1301 | 0.0863 | 0.8548 | 0.5630 | 0.0451 |
| Volcanic | **NH volcanic aerosol** | 19 | -0.0700 | 0.7758 | 0.1305 | 0.5945 | 0.1595 | 0.0963 | 0.6951 |
| | **Global volcanic aerosol** | 19 | 0.0647 | 0.7924 | 0.277 | 0.2507 | 0.0478 | 0.2528 | 0.2965 |
| | ***Global volcanic forcing** | 16 | 0.3170 | 0.2316 | 0.2549 | 0.2923 | 0.1945 | 0.1358 | 0.5795 |
| North Atlantic modes | **NAO** | 16 | 0.0999 | 0.7127 | 0.3315 | 0.2098 | 0.3004 | 0.2312 | 0.3890 |
| | **AMO** | 19 | 0.6022 | 0.0064 | 0.3732 | 0.1156 | 0.4841 | 0.2547 | 0.2928 |
| Greenhouse gases | **$CO_2$ (ppm)** | 20 | 0.7364 | 0.0002 | 0.7293 | 0.0003 | 0.9741 | 0.6529 | 0.0018 |
| | **$NO_2$ (ppm)** | 20 | 0.6538 | 0.0018 | 0.6846 | 0.0009 | 0.9225 | 0.6102 | 0.0043 |
| | **$CH_4$ (ppm)** | 20 | 0.7285 | 0.0003 | 0.7737 | 0.0001 | 0.3468 | 0.7071 | 0.0005 |
| Temperatures | **CPS Summer temperatures** | 20 | 0.7071 | 0.0005 | 0.4586 | 0.0420 | 0.1835 | 0.3403 | 0.1421 |
| | **SST uk37 Gol-Ho1B** | 20 | 0.6097 | 0.0043 | 0.7254 | 0.0003 | 0.1192 | 0.6519 | 0.0018 |
| | **SST uk37 TTR-17-1-384B** | 17 | 0.2378 | 0.3581 | 0.0206 | 0.9374 | 0.7731 | 0.0152 | 0.9537 |
| | **SST TEX86 TTR-17-384B** | 17 | 0.4489 | 0.0707 | 0.5265 | 0.0299 | 0.9671 | 0.4754 | 0.0538 |
| | **SST uk37 TTR-17-1-436B** | 18 | 0.3383 | 0.1697 | 0.6774 | 0.0020 | 0.3247 | 0.6989 | 0.0013 |
| | **SST TEX86 TTR-17-436B** | 18 | 0.4338 | 0.0721 | 0.1767 | 0.4830 | 0.4047 | 0.3449 | 0.1610 |

**Supplementary Table S6.** Pearson correlations (normal and detrended) between LdRS long core LDI record and different proxies for solar and volcanic forcing, North Atlantic modes, greenhouse gases, and temperatures. Normal correlations show long-term trends. Data were standardised (z-scores), normalised (squares), and a Mann-Kendall trend test was performed using PAST software (Hammer et al., 2001) in order to assess the existence of any trend over time in the data series. Afterwards, data were detrended by fitting a linear regression versus time, and a Pearson correlation was worked out with the residuals. *****: Note that inverse $\Delta^{14}C$ and global volcanic forcing values have been used in order to show the same trends as in Fig. 4.

**Solar Proxies:** **$\Delta^{14}C$** (Reimer et al., 2013); ΔTSI, reconstruction of the difference of the total solar irradiance from the value of the PMOD composite series during the solar cycle minimum of the year 1986 CE (1365.57 W $m^{-2}$) (Steinhilber et al., 2009); TSI, total solar irradiance (Coddington et al., 2016).

**Volcanic proxies:** Annual stratospheric volcanic sulfate aerosol injection for the past 1500 years in the North Hemisphere, and worldwide (Gao et al., 2008); global volcanic aerosol forcing (W $m^{-2}$) (Sigl et al., 2015).

**North Atlantic modes:** NAO, North Atlantic Oscillation reconstruction (Trouet et al., 2009); AMO, Atlantic Multidecadal Oscillation reconstruction (Mann et al., 2009).

**Greenhouse gases**: reconstructed concentrations of atmospheric $CO_2$, $NO_2$, and $CH_4$ (ppm) (Schmidt et al., 2011).

**Temperatures:** Composite-plus-scaling (CPS) mean summer temperature anomaly reconstruction from tree rings records in Europe with respect to 1974-2003 CE (MSTA ºC) (Luterbacher et al., 2016); Alkenone-Sea Surface Temperatures (SST ºC) of the core Gol-Ho1B_KSGC-31 (Gulf of Lion: NW Mediterranean Sea) (Sicre et al., 2016), alkenone and $TEX_{86}$ (from GDGTs) SST records of the cores 384B and 436B in the Alboran Sea (Nieto-Moreno et al., 2013).

| Record | Lab Code | Sampling Depth (cm) | Cal yr BP | Yr CE | $C_{28}$ 1,13-diol | $C_{30}$ 1,15-diol | $C_{30}$ 1,13-diol | $C_{32}$ 1,15-diol | LDI | Observations |
|---|---|---|---|---|---|---|---|---|---|---|
| LdRS shc | BECS 1271 | 0 | -58 | 2008 | 0.0449 | 0.0506 | 0.0807 | 0.8238 | 0.2871 | |
| LdRS shc | BECS 1272 | 0.5 | -53 | 2003 | 0.0598 | 0.0590 | 0.0772 | 0.8040 | 0.3012 | |
| LdRS shc | BECS 1273 | 1 | -48 | 1998 | 0.0525 | 0.0620 | 0.0792 | 0.8063 | 0.3202 | |
| LdRS shc | BECS 1274 | 1.5 | -43 | 1993 | 0.0539 | 0.0568 | 0.0893 | 0.8000 | 0.2840 | |
| LdRS shc | BECS 1275 | 2 | -38 | 1988 | 0.0721 | 0.0584 | 0.1060 | 0.7635 | 0.2470 | |
| LdRS shc | BECS 1276 | 2.5 | -33 | 1983 | 0.0579 | 0.0600 | 0.1032 | 0.7789 | 0.2713 | |
| LdRS shc | BECS 1277 | 3 | -28 | 1978 | 0.0805 | 0.0639 | 0.1043 | 0.7513 | 0.2569 | |
| LdRS shc | BECS 1278 | 3.5 | -23 | 1973 | 0.0676 | 0.0601 | 0.1174 | 0.7549 | 0.2452 | |
| LdRS shc | BECS 1279 | 4 | -18 | 1968 | 0.0789 | 0.0611 | 0.1232 | 0.7368 | 0.2320 | |
| LdRS shc | BECS 1280 | 4.5 | -13 | 1963 | 0.0863 | 0.0635 | 0.1313 | 0.7189 | 0.2260 | |
| LdRS shc | BECS 1281 | 5 | -8 | 1958 | 0.0801 | 0.0664 | 0.1308 | 0.7227 | 0.2395 | |
| LdRS shc | BECS 1282 | 5.5 | -3 | 1953 | 0.0819 | 0.0667 | 0.1341 | 0.7173 | 0.2359 | |
| LdRS shc | BECS 1283 | 6 | 2 | 1948 | 0.0934 | 0.0564 | 0.1323 | 0.7180 | 0.1999 | |
| LdRS shc | BECS 1284 | 6.5 | 9 | 1941 | 0.1281 | 0.0549 | 0.1492 | 0.6678 | 0.1654 | |
| LdRS shc | BECS 1285 | 7 | 15 | 1935 | 0.1233 | 0.0563 | 0.1531 | 0.6674 | 0.1693 | |
| LdRS shc | BECS 1286 | 7.5 | 22 | 1928 | 0.1067 | 0.0525 | 0.1389 | 0.7019 | 0.1762 | |
| LdRS shc | BECS 1322 | 8 | 29 | 1921 | 0.1193 | 0.0485 | 0.1576 | 0.6746 | 0.1492 | |
| LdRS shc | BECS 1323 | 8.5 | 35 | 1915 | 0.1326 | 0.0492 | 0.1742 | 0.6441 | 0.1382 | |
| LdRS shc | BECS 1324 | 9 | 42 | 1908 | 0.1508 | 0.0489 | 0.1800 | 0.6203 | 0.1288 | |
| LdRS shc | BECS 1325 | 9.5 | 49 | 1901 | 0.1345 | 0.0468 | 0.1782 | 0.6405 | 0.1302 | |
| LdRS shc | BECS 1326 | 10 | 55 | 1895 | 0.1446 | 0.0475 | 0.1724 | 0.6354 | 0.1304 | |
| LdRS shc | BECS 1327 | 10.5 | 62 | 1888 | 0.1315 | 0.0501 | 0.1645 | 0.6538 | 0.1448 | |
| LdRS shc | BECS 1328 | 11 | 69 | 1881 | 0.1429 | 0.0508 | 0.1705 | 0.6357 | 0.1396 | |
| LdRS shc | BECS 1329 | 11.5 | 75 | 1875 | 0.1306 | 0.0509 | 0.1713 | 0.6472 | 0.1443 | |
| LdRS shc | BECS 1330 | 12 | 82 | 1868 | 0.1184 | 0.0524 | 0.1738 | 0.6555 | 0.1520 | |
| LdRS shc | BECS 1331 | 12.5 | 89 | 1861 | 0.1171 | 0.0491 | 0.1879 | 0.6460 | 0.1386 | |
| LdRS shc | BECS 1332 | 13 | 95 | 1855 | 0.1132 | 0.0515 | 0.1961 | 0.6393 | 0.1426 | |
| LdRS shc | BECS 1333 | 13.5 | 102 | 1848 | 0.0918 | 0.0573 | 0.1705 | 0.6804 | 0.1792 | |
| LdRS shc | BECS 1334 | 14 | 109 | 1841 | 0.0852 | 0.0607 | 0.1660 | 0.6881 | 0.1945 | |
| LdRS shc | BECS 1335 | 14.5 | 115 | 1835 | 0.0741 | 0.0621 | 0.1597 | 0.7041 | 0.2098 | |
| LdRS shc | BECS 1336 | 15 | 122 | 1828 | 0.0755 | 0.0625 | 0.1649 | 0.6972 | 0.2064 | |
| LdRS shc | BECS 1337 | 15.5 | 129 | 1821 | 0.0746 | 0.0596 | 0.1746 | 0.6912 | 0.1930 | |
| LdRS lgc | GMOL 1886 | 0 | -56 | 2006 | 0.0708 | 0.0703 | 0.1041 | 0.7548 | 0.2866 | |
| LdRS lgc | GMOL 1887 | 1 | -41 | 1991 | 0.0630 | 0.0742 | 0.1032 | 0.7596 | 0.3087 | |
| LdRS lgc | GMOL 1888 | 2 | -26 | 1976 | 0.1016 | 0.0765 | 0.1399 | 0.6820 | 0.2405 | |
| LdRS lgc | GMOL 1889 | 3 | -11 | 1961 | 0.1264 | 0.0796 | 0.1585 | 0.6356 | 0.2183 | |
| LdRS lgc | GMOL 1890 | 4 | 4 | 1946 | 0.2003 | 0.0647 | 0.1724 | 0.5625 | 0.1479 | |
| LdRS lgc | GMOL 1891 | 5 | 20 | 1931 | 0.1477 | 0.0620 | 0.1338 | 0.6566 | 0.1805 | |
| LdRS lgc | GMOL 1892 | 6 | 35 | 1915 | 0.2733 | 0.0516 | 0.1666 | 0.5085 | 0.1049 | |
| LdRS lgc | GMOL 1893 | 7 | 50 | 1900 | 0.2283 | 0.0623 | 0.1911 | 0.5183 | 0.1294 | |

| | | | | | | | | | | |
|---|---|---|---|---|---|---|---|---|---|---|
| LdRS lgc | GMOL 1895 | 9 | 80 | 1870 | 0.1334 | 0.0586 | 0.2003 | 0.6076 | 0.1495 | |
| LdRS lgc | GMOL 1896 | 10.5 | 106 | 1844 | 0.1093 | 0.0644 | 0.1937 | 0.6326 | 0.1752 | |
| LdRS lgc | GMOL 1897 | 11.5 | 169 | 1781 | 0.4216 | 0.0551 | 0.1927 | 0.3307 | 0.0823 | |
| LdRS lgc | GMOL 1898 | 12.5 | 263 | 1687 | 0.4132 | 0.0325 | 0.1851 | 0.3692 | 0.0515 | |
| LdRS lgc | GMOL 1899 | 13.5 | 343 | 1607 | 0.3809 | 0.0578 | 0.3068 | 0.2545 | 0.0775 | |
| LdRS lgc | GMOL 1900 | 14.5 | 437 | 1513 | 0.3456 | 0.0603 | 0.2828 | 0.3113 | 0.0876 | |
| LdRS lgc | GMOL 1901 | 15.5 | 547 | 1403 | 0.2543 | 0.0923 | 0.2568 | 0.3966 | 0.1529 | |
| LdRS lgc | GMOL 1902 | 16.5 | 738 | 1212 | 0.1883 | 0.0859 | 0.1677 | 0.5581 | 0.1944 | |
| LdRS lgc | GMOL 1903 | 17.5 | 876 | 1074 | 0.2448 | 0.0732 | 0.2179 | 0.4641 | 0.1366 | |
| LdRS lgc | GMOL 1904 | 18.5 | 1022 | 928 | 0.1784 | 0.1070 | 0.1753 | 0.5394 | 0.2322 | |
| LdRS lgc | GMOL 1905 | 19.5 | | | | | | | | below quantification limits |
| LdRS lgc | GMOL 1906 | 20.5 | 1404 | 546 | 0.2144 | 0.0938 | 0.2602 | 0.4316 | 0.1650 | |
| LdRS lgc | GMOL 1907 | 21.5 | 1556 | 394 | 0.2210 | 0.0878 | 0.2165 | 0.4746 | 0.1672 | |

**Supplementary Table S7.** Fractional abundances of $C_{28}$ 1,13-diol, $C_{30}$ 1,13-diol, $C_{30}$ 1,15-diol, and $C_{32}$ 1,15-diol in the different samples of both LdRS cores (LdRS shc and LdRS lgc) along with the obtained Long Chain Diol Index (LDI), according to Rampen et al. (2012).

## Supplementary References


Barea-Arco, J., Pérez-Martínez, C., and Morales-Baquero, R.: Evidence of a mutualistic relationship between an algal epibiont and its host, Daphnia pulicaria, Limnology and Oceanography, 46, 871-881, 2001.

Carrillo, P., Cruz-Pizarro, L., and Sánchez Castillo, P. M.: Aportación al conocimiento del ciclo biológico de Chromulina nevadensis, Acta Botánica Malacitana, 16, 19-26, 1991.

Coddington, O., Lean, J. L., Pilewskie, P., Snow, M., and Lindholm, D.: A Solar Irradiance Climate Data Record, Bulletin of the American Meteorological Society, 97, 1265-1282, 10.1175/bams-d-14-00265.1, 2016.

Dogniaux, R.: Prediction of Solar Radiation in Areas with a Specific Microclimate, Prediction of Solar Radiation in Areas with a Specific Microclimate, 108 pp., 1994.

Gao, C., Robock, A., and Ammann, C.: Volcanic forcing of climate over the past 1500 years: An improved ice core-based index for climate models, Journal of Geophysical Research: Atmospheres, 113, doi:10.1029/2008JD010239, 2008.

Gonzalez-Hidalgo, J. C., Peña-Angulo, D., Brunetti, M., and Cortesi, N.: MOTEDAS: a new monthly temperature database for mainland Spain and the trend in temperature (1951–2010), International Journal of Climatology, 35, 4444-4463, 10.1002/joc.4298, 2015.

Hammer, Ø., Harper, D. A. T., and Ryan, P. D.: PAST: Paleontological statistics software package for education and data analysis, Palaeontologia Electronica 4, 9, 2001.

Hansen, J., Ruedy, R., Sato, M., and Lo, K.: Global Surface Temperature Change, Reviews of Geophysics, 48, 10.1029/2010RG000345, 2010.

Luterbacher, J., Werner, J. P., Smerdon, J. E., Fernández-Donado, L., González-Rouco, F. J., Barriopedro, D., Ljungqvist, F. C., Büntgen, U., Zorita, E., Wagner, S., Esper, J., McCarroll, D., Toreti, A., Frank, D., Jungclaus, J. H., Barriendos, M., Bertolin, C., Bothe, O., Brázdil, R., Camuffo, D., Dobrovolný, P., Gagen, M., García-Bustamante, E., Ge, Q., Gómez-Navarro, J. J., Guiot, J., Hao, Z., Hegerl, G. C., Holmgren, K., Klimenko, V. V., Martín-Chivelet, J., Pfister, C., Roberts, N., Schindler, A., Schurer, A., Solomina, O., von Gunten, L., Wahl, E., Wanner, H., Wetter, O., Xoplaki, E., Yuan, N., Zanchettin, D., Zhang, H., and Zerefos, C.: European summer temperatures since Roman times, Environmental Research Letters, 11, 024001, citeulike-article-id:14089240 doi: 10.1088/1748-9326/11/2/024001, 2016.

Mann, M. E., Zhang, Z., Rutherford, S., Bradley, R. S., Hughes, M. K., Shindell, D., Ammann, C., Faluvegi, G., and Ni, F.: Global Signatures and Dynamical Origins of the Little Ice Age and Medieval Climate Anomaly, Science, 326, 1256-1260, 10.1126/science.1177303, 2009.

Nieto-Moreno, V., Martínez-Ruiz, F., Willmott, V., García-Orellana, J., Masqué, P., and Sinninghe Damsté, J. S.: Climate conditions in the westernmost Mediterranean over the last two millennia: An integrated biomarker approach, Organic Geochemistry, 55, 1-10, https://doi.org/10.1016/j.orggeochem.2012.11.001, 2013.

Organization, I. C. A.: Manual of the ICAO standard atmosphere : extended to 80 kilometres (262 500 feet) (Third ed.), International Civil Aviation Organization, Montreal, Quebec, 1993.

Reimer, P. J., Bard, E., Bayliss, A., Beck, J. W., Blackwell, P. G., Ramsey, C. B., Buck, C. E., Cheng, H., Edwards, R. L., Friedrich, M., Grootes, P. M., Guilderson, T. P., Haflidason, H., Hajdas, I., Hatté, C., Heaton, T. J., Hoffmann, D. L., Hogg, A. G., Hughen, K. A., Kaiser, K. F., Kromer, B., Manning, S. W., Niu, M., Reimer, R. W., Richards, D. A., Scott, E. M., Southon, J. R., Staff, R. A., Turney, C. S. M., and van der Plicht, J.: IntCal13 and Marine13 Radiocarbon Age Calibration Curves 0–50,000 Years cal BP, Radiocarbon, 55, 1869-1887, https://doi.org/10.2458/azu_js_rc.55.16947, 2013.

Sánchez-Castillo, P. M.: Algas de las lagunas de alta montaña de Sierra Nevada (Granada, España), Acta Botánica Malacitana, 13, 21 -52, 1988.

Sandgren, C. D.: The ecology of chrysophyte flagellates: their growth and perennation strategies as freshwater phytoplankton, in: Growth and reproductive strategies of freshwater phytoplankton, edited by: C.D., S., Cambridge University Press, Cambridge, 9-104, 1988.

Schmidt, G. A., Jungclaus, J. H., Ammann, C. M., Bard, E., Braconnot, P., Crowley, T. J., Delaygue, G., Joos, F., Krivova, N. A., Muscheler, R., Otto-Bliesner, B. L., Pongratz, J., Shindell, D. T., Solanki, S. K., Steinhilber, F., and Vieira, L. E. A.: Climate forcing reconstructions for use in PMIP simulations of the last millennium (v1.0), Geosci. Model Dev., 4, 33-45, 10.5194/gmd-4-33-2011, 2011.

Sicre, M.-A., Jalali, B., Martrat, B., Schmidt, S., Bassetti, M.-A., and Kallel, N.: Sea surface temperature variability in the North Western Mediterranean Sea (Gulf of Lion) during the Common Era, Earth and Planetary Science Letters, 456, 124-133, https://doi.org/10.1016/j.epsl.2016.09.032, 2016.

Sigl, M., Winstrup, M., McConnell, J. R., Welten, K. C., Plunkett, G., Ludlow, F., Buntgen, U., Caffee, M., Chellman, N., Dahl-Jensen, D., Fischer, H., Kipfstuhl, S., Kostick, C., Maselli, O. J., Mekhaldi, F., Mulvaney, R., Muscheler, R., Pasteris, D. R., Pilcher, J. R., Salzer, M., Schupbach, S., Steffensen, J. P., Vinther, B. M., and Woodruff, T. E.: Timing and climate forcing of volcanic eruptions for the past 2,500 years, Nature, 523, 543-549, 10.1038/nature14565 http://www.nature.com/nature/journal/v523/n7562/abs/nature14565.html#supplementary-information, 2015.

Steinhilber, F., Beer, J., and Fröhlich, C.: Total solar irradiance during the Holocene, Geophysical Research Letters, 36, 10.1029/2009GL040142, 2009.

Trouet, V., Esper, J., Graham, N. E., Baker, A., Scourse, J. D., and Frank, D. C.: Persistent Positive North Atlantic Oscillation Mode Dominated the Medieval Climate Anomaly, Science, 324, 78-80, 10.1126/science.1166349, 2009.